HHS Public Access

Author manuscript

J Psychiatr Res. Author manuscript; available in PMC 2018 June 01.

Published in final edited form as:

J Psychiatr Res. 2017 June ; 89: 85–96. doi:10.1016/j.jpsychires.2017.01.018.

Nicotinic modulation of salience network connectivity and centrality in schizophrenia

Jason Smucny, M.S.[1,3], **Korey P. Wylie, M.D.**[3], **Eugene Kronberg, Ph.D.**[3], **Kristina T. Legget, Ph.D.**[1,2,3], and **Jason R. Tregellas, Ph.D.**[1,2,3]

[1]Neuroscience Program, University of Colorado Anschutz Medical Campus, Aurora CO USA

[2]Research Service, Denver VA Medical Center, Denver, CO USA

[3]Department of Psychiatry, University of Colorado Anschutz Medical Campus, Aurora CO USA

Abstract

Although functional abnormalities of the salience network are associated with schizophrenia, the acute effects of nicotine on its function and network dynamics during the resting state in patients are poorly understood. In this study, the effects of a 7 mg nicotine patch (vs. placebo) on salience network connectivity were examined in 17 patients with schizophrenia and 19 healthy subjects. We hypothesized abnormal connectivity between the salience network and other major networks (e.g. executive network) in patients under placebo administration and amelioration of this difference after nicotine. We also examined effects of nicotine on betweenness centrality (a measure of the influence of a region on information transfer throughout the brain) and local efficiency (a measure of local information transfer) of the network. A hybrid independent component analysis (ICA) / seed-based connectivity approach was implemented in which the salience network was extracted by ICA and cortical network peaks (anterior cingulate cortex (ACC), left and right insula) were used as seeds for whole-brain seed-to-voxel connectivity analysis. Significant drug X diagnosis interactions were observed between the ACC seed and superior parietal lobule and ventrolateral prefrontal cortex. A significant interaction effect was also observed between the left insula seed and middle cingulate cortex. During placebo conditions, abnormal connectivity predicted negative symptom severity and lower global functioning in patients. A significant drug X diagnosis interaction was also observed for betweenness centrality of the ACC. These results suggest that nicotine may target abnormalities in functional connectivity between salience and executive network areas in schizophrenia as well as affect the ability of the salience network to act as an integrator of global signaling in the disorder.

Compliance with Ethical Standards

All procedures performed in studies involving human participants were in accordance with the ethical standards of the institutional and/or national research committee and with the 1964 Helsinki declaration and its later amendments or comparable ethical standards. Informed consent was obtained from all individual participants included in the study. Subjects could withdraw from the study at any time and were compensated for participation. The Colorado Multiple Institutional Review Board approved the study. The authors declare no conflicts of interest in relation to this work.

Keywords

Anterior Cingulate; Betweenness Centrality; Insula; Nicotine; Resting State; Schizophrenia

Introduction

The brain is constantly bombarded by information from the external environment and internal sources. In order to produce an appropriate response and form a coherent experience of the world (i.e. our concept of "reality") the brain must be able to constantly filter, integrate, and evaluate this information. This moment-to-moment evaluation is a major function of the salience network, a functionally (Menon, 2015) and structurally (Uddin et al., 2011; van den Heuvel et al., 2009) connected set of brain areas that includes the anterior insular and anterior cingulate cortices (ACC). The salience network is able to accomplish this task through its functional connectivity to diverse brain areas. These include regions involved in executive function (e.g. prefrontal cortex and superior parietal cortex) as well as to areas that comprise the "default mode network" (DMN) (e.g. posterior cingulate cortex, inferior parietal cortices and preceneus) (Menon and Uddin, 2010). Indeed, due to its patterns of intrinsic connectivity, the salience network may be involved in switching between executive and default-mode dominant states based on task demands (Menon, 2011; Menon and Uddin, 2010; Palaniyappan and Liddle, 2012).

Given that the salience network may play a key role in how we perceive the world and consequently shape our reality, it perhaps comes as no surprise that dysfunction of the network is increasingly believed to play a cardinal role in psychosis and schizophrenia. Indeed, salience network dysfunction may also play a critical role in explaining the negative and cognitive symptoms of the illness. Cognitive symptoms may involve the inability to appropriately switch between networks. Negative symptoms suggest that patients are unable to act appropriately based on circumstances. In support of this view, previous work has demonstrated that the salience network is functionally, structurally, and neurochemically abnormal in schizophrenia (reviewed by Palaniyappan and Liddle (2012); Palaniyappan et al. (2012); Smucny and Tregellas (2013); Wylie and Tregellas (2010)). Resting-state functional magnetic resonance imaging (fMRI) studies have reported abnormal salience network connectivity in schizophrenia, including within the network (Kraguljac et al., 2016; Pu et al., 2012) and between the network and other networks (Manoliu et al., 2014; Moran et al., 2013b; Palaniyappan et al., 2013; Pelletier-Baldelli et al., 2015). Finally, salience network dysfunction has been linked to all three domains of symptoms in schizophrenia (Kuhn and Gallinat, 2012; Lahti et al., 2006; Manoliu et al., 2013; Palaniyappan et al., 2013).

Given that the salience network may play a key role in understanding the symptoms of schizophrenia, it follows that pharmacologically targeting the network may have clinical utility. One highly studied class of drugs in schizophrenia is nicotinic agonists. Interest in these drugs is due to high rates of smoking (~70%) in the illness (Winterer, 2010) leading researchers to hypothesize that nicotine may be a form of "self medication" (Winterer, 2010). In schizophrenia, acute nicotine has been shown to improve cognition as well as

target abnormal brain function (Barr et al., 2008; Harris et al., 2004; Smucny et al., 2016a; Smucny et al., 2016b; Smucny et al., 2015; Tregellas et al., 2011; Wylie et al., 2016). Conversely, the nicotinic antagonist mecamylamine worsens cognitive performance in patients (Roh et al., 2014). Aberrant salience network function is associated with smoking status in schizophrenia (Moran et al., 2013a), targeted by nicotine in healthy deprived cigarette smokers (Hong et al., 2009; Sutherland et al., 2013), and may be a critical system underlying nicotine addition (reviewed by Sutherland et al., 2012). Finally, all three nodes of the salience network highly express nicotinic receptors (Breese et al., 1997; Paterson and Nordberg, 2000; Picard et al., 2013), suggesting the network may be effectively targeted by nicotine and other nicotinic agents.

To examine the effects of pharmacologic treatment on brain network connectivity, researchers most frequently adopt seed-based (connectivity between a seed and other regions) or multivariate (e.g. independent components analysis (ICA)) approaches. To take these analyses a step further, topological analysis or “graph theory” can be used to ascertain the organizational principles that underlie functional intrinsic networks. One interesting topological metric is *betweenness centrality*, a term that describes how frequently a brain region is used to enable one area to communicate with another. A node (e.g. brain region) with high betweenness centrality is frequently used to traverse from any region in a network of brain regions to any other region (Fig. 1, top). Related to this point, the relatively high betweenness centrality of the salience network may drive its ability to integrate information and process salience (van den Heuvel and Sporns, 2013). Furthermore, previous studies suggest that betweenness centrality of the ACC may be disrupted in schizophrenia and in at-risk populations (Lord et al., 2012; Lord et al., 2011; van den Heuvel et al., 2010).

In contrast to betweenness centrality, analysis of *local efficiency* examines communication solely between a node (e.g. brain region) and its “neighbors” (other regions directly connected to that region) and is therefore a measure of local (rather than global) information integration. Neighbors surrounding a node with high local efficiency are able to communicate between themselves without having to traverse between many other nodes (Fig. 1, bottom). Disrupted local efficiency has been observed in schizophrenia patients in a number of areas, including the ACC (Smucny and Tregellas, 2013; Yan et al., 2015).

Despite the links between the salience network, schizophrenia, and nicotine, little is known about the effects of the drug on salience network connectivity and topology in the illness, particularly in nonsmokers. Filling in this knowledge gap is important as a substantial fraction (~30%) of schizophrenia patients do not smoke (Winterer, 2010). Studying nonsmokers, furthermore, circumvents the unavoidable confounding effects of withdrawal associated with studying a smoking population. The goals of this study, therefore, were to 1) examine the effects of acute nicotine administration (vs. placebo) on connectivity between the three cortical nodes of the salience network (ACC, left and right anterior insula) and the rest of the brain in patients, and 2) examine the effects of nicotine (vs. placebo) on betweenness centrality and local efficiency of the three salience network nodes. We hypothesized abnormal connectivity between the salience network and brain regions associated with other major networks (e.g. the prefrontal cortex/executive network) as well

as disrupted betweenness centrality and local efficiency of salience network nodes in patients under placebo administration and amelioration of these differences after nicotine.

Materials and Methods

Subjects

36 subjects participated in this study — 17 stable outpatients who had a primary diagnosis of schizophrenia and 19 healthy comparison subjects. Demographic and clinical (Brief Psychiatric Rating Scale (BPRS, 24 point) (Ventura et al., 1993), Scale for the Assessment of Negative Symptoms (SANS, 4 factor) (Andreasen, 1983), and Global Assessment of Function (GAF) (Jones et al., 1995)) information for participants was assessed by interview and is shown in Table 1. No significant group differences in age or gender were observed. No subjects were taking smoking cessation medication (e.g. varenicline) at the time of the study. Controls were recruited by advertisement. Patients were recruited by referral from a University of Colorado psychiatrist. Patients were excluded for a diagnosis of neurological illness, head trauma, current smoking (< 3 months from last cigarette) or substance abuse, failure to pass a physical examination, and magnetic resonance imaging (MRI) exclusion criteria (claustrophobia, weight > 250 pounds, metal in the body). Control subjects were excluded for all of the above as well as a diagnosis of Axis I mental illness or first-degree family history of Axis I mental illness. No significant difference between groups in the ratio of never smokers to former smokers was observed. Importantly, increased nicotinic receptor expression levels (tied to smoking) have been shown to normalize by 6 weeks in former smokers (Cosgrove et al., 2009). Patients were antipsychotic medication stable (> 3 months with no change in medication; see Supplementary Table 1 for a listing of antipsychotic medication(s) taken by patients at the time of the study). All subjects were required to pass a nicotine tolerance test, in which the nicotine dose used for the experiment (7 mg) was administered > 3 days prior to the first fMRI scan. Criteria for passing the tolerance test were 1) less than a 20% change in heart rate or blood pressure (BP) for up to 90 minutes post patch-application, 2) no side effects other than mild/minor nausea, headache, lightheadness, clouded thinking, anxiety, or mouth tingling.

Study Design and Drug Administration

This was a single-blind, randomized, placebo-controlled, crossover study. On each of two study visits, subjects were administered either a 7 mg nicotine patch (NicoDerm CQ, GlaxoSmithKline, Middlesex, UK) or placebo patch (made in-house). The order of study visits (placebo-nicotine or nicotine-placebo) was counterbalanced across subjects. Visits were scheduled more than 3 days apart. The placebo and nicotine patches were tactilely identical, and the placebo patch was affixed to the skin in the same manner as the nicotine patch. Subjects were asked to refrain from examining either patch, however, during or after application as the placebo and drug patches (although visually similar) were not visually identical. Participants' clothing (sleeves) also covered the patches such that they could not be readily observed after affixation. Patches remained affixed from application to the end of the scan.

Resting-state scans were performed approximately 120 minutes after patch application. The latent period for this study and our previously published attention studies (Smucny et al., 2016a; Smucny et al., 2016b) was used such that the scans are anticipated to occur during a time window corresponding to the peak plasma concentration of nicotine (Dempsey et al., 2013). Total scan time (including high order shimming, T1 scan, and attention and listening tasks preceding the resting state scan) was 60 minutes. Based on previous work, the nicotine concentration during this period is expected to be approximately 4.5 ng/ml (Dempsey et al., 2013).

Physiological effects (heart rate (HR) and blood pressure (BP)) were monitored immediately prior to 1) patch application and 2) entering the MR scanner. Physiological effects were analyzed using a mixed-effects model analysis of variance (ANOVA) in SPSS v. 22 (IBM Corp., Armonk, NY, USA), with time (pretreatment vs. posttreatment) and drug (placebo vs. nicotine) as within-subjects factors and diagnosis (control vs. patient) as a between-subjects factor.

fMRI Acquisition

Resting state functional images were acquired on a 3T MR scanner (General Electric, Milwaukee, WI, USA) using a standard quadrature head coil. An inversion-recovery echoplanar image (IR-EPI; TI = 505 ms) was collected to improve coregistration of functional images. Images were acquired with the following parameters: scan time 10 minutes, TR = 2000 ms, TE = 26 ms, FOV = 220 mm^2, 64^2 matrix, 27 slices, 2.6 mm thick, 1.4 mm gap, interleaved, flip angle 70°, 300 volumes. Subjects were instructed to rest with eyes closed, to not fall asleep, and to “not think about anything in particular.” Although having subjects rest with eyes closed potentially induces variable levels of drowsiness during the scan, previous work suggests that only auditory network connectivity is affected by having subjects rest with eyes closed vs. eyes open (Patriat et al., 2013).

fMRI Preprocessing – Realignment, Coregistration and Smoothing

fMRI data realignment, coregistration and smoothing were performed using SPM8 (Wellcome Dept. of Imaging Neuroscience, London) in Matlab 2012a (MathWorks, Natick, MA, USA). The first four images were excluded for saturation effects. Data from each subject were realigned to the first volume and normalized to the Montreal Neurological Institute template using the IR-EPI as an intermediate to improve coregistration between images. During spatial normalization, data were resliced to a 3 mm^3 voxel size. Finally, data were smoothed with an 8 mm full width half maximum (FWHM) Gaussian kernel.

Functional Connectivity Analysis

A hybrid ICA / seed-based connectivity approach was utilized (Kelly et al., 2010). This methodology first uses ICA to extract group level networks of interest (in this study, the salience network). Focal signal peaks from that network are then used as seeds in a whole-brain seed-to-voxel connectivity analysis. This approach provides a data-driven, unbiased estimate of connectivity between specific regions within the salience network and the rest of the brain, as it does not require prespecification of anatomically-based seeds of unknown reliability and validity (Zilles and Amunts, 2010). Importantly, no statistical analysis was

performed on ICA results to avoid potentially performing circular analyses (i.e. “double dipping”) (Kriegeskorte et al., 2009). Details of each step of the hybrid procedure will be discussed in the proceeding sections.

Preprocessing—Preprocessing for connectivity analysis was conducted using in-house Matlab 2012a scripts according to suggested guidelines (Murphy et al., 2013). White matter and CSF signals were included as covariates of no interest (confounders). BOLD response associated with the main effect of drug was also removed in order to obtain an estimate of connectivity independent of activation. Mean overall gray matter signal was not included as a confounder as doing so shifted the whole-brain connectivity distribution towards predominantly negative values. The data were linearly detrended and a 0.01 to 0.1 Hz bandpass filter applied to remove low-frequency drifts and physiological high-frequency noise.

Subject motion has been shown to affect functional connectivity (Power et al., 2012). To mitigate these effects, rigid-body motion parameters (left/right (x translation), forward/back (y translation), up/down (z translation), pitch (lateral rotation parameter), yaw (perpendicular rotation parameter) and roll (longitudinal rotation parameter)) were first included as covariates of no interest (average values presented in Supplementary Table 2). Censoring was then performed in which adjacent volumes that showed scan-to-scan differences of > 0.5 mm (translational displacement), > 0.2 rad (rotational displacement), or > 9 (global signal z-value) were removed before analysis. Significant main effects or interaction effects were observed for several movement parameters as well as variance of global signal, resulting in differences in the number of frames scrubbed between groups (Supplementary Table 2). All subjects, however, still had < 50% of frames removed after censoring, and the mean number of frames scrubbed per group was low for all groups (<5%). Censoring was performed using the ART toolbox (www.nitrc.org/projects/artifact_detect).

ICA—Group spatial ICA was performed using the GIFT software v1.3g (icatb.sourceforge.net). A single group ICA was performed across all subjects (controls and patients) and treatment conditions (placebo and nicotine). ICA parameters have been described previously (Tregellas et al., 2014). Briefly, data were intensity-normalized, their dimensionality reduced using principle component analysis, and twenty independent sources estimated using the Infomax algorithm (Bell and Sejnowski, 1995). The component containing the salience network was identified by selecting the component with the highest spatial correlation with an anterior salience network mask (Shirer et al., 2012). Consistent with previous ICA findings (Seeley et al., 2007; Sridharan et al., 2008), the extracted network included the left and right anterior insula as well as the ACC (Fig. 2, top). The extracted peak coordinates were $\{x, y, z\} = \{-42, 20, 5\}$ (left insula), {39, 26, −8} (right insula), {−3, 17, 58} (dorsal ACC). These seed regions are spatially similar to salience network nodes recently identified during a risky decision-making task (Wei et al., 2016). Consequently, 5 mm radius spherical ROIs were centered on these peaks and used as seeds for whole brain seed-to-voxel connectivity analysis (Kelly et al., 2010) (Fig. 2, bottom).

Whole Brain Seed-to-Voxel Connectivity Analysis—Seed-based connectivity analysis was performed using the Conn v.15 toolbox (www.nitrc.org/projects/conn). Second-level random effects mixed-model ANOVA analyses were performed to examine connectivity differences between groups. For these analyses, treatment condition (placebo vs. nicotine) was entered as a within-subjects factor and diagnosis (control vs. patient) was entered as a between-subjects factor. The primary contrasts of interest were the directional interaction contrast (Patient Nicotine > Patient Placebo) > (Control Nicotine > Control Placebo) (i.e. increased connectivity during nicotine administration (vs. placebo) in patients vs. control) and the opposite interaction contrast (Patient Placebo > Patient Nicotine) > (Control Placebo > Control Nicotine) (i.e. decreased connectivity during nicotine administration (vs. placebo) in patients vs. control). Second-level connectivity maps were thresholded at $p < 0.01$ (voxelwise), $q < 0.01$ (cluster false discovery rate-corrected voxels) in SPM8 (Genovese et al., 2002). To fully characterize interaction effects, significant interactions were followed up by post-hoc tests of simple main effects using the mean connectivity between the seed and each significant cluster, as described previously (Dodhia et al., 2014).

Topological Analysis

Betweenness centrality and local efficiency are analyzed in a topological framework, in which the brain is parcellated into anatomically defined regions, or “nodes”, and metrics calculated for ROIs (in this study, the ROIs consisted of the three salience network peaks described previously). Connectivity between nodes is then calculated to provide the basis for drawing “edges” (lines representing connections) of the graph. The proceeding sections provide a step-by-step description of the procedures used in these analyses. All calculations were performed using the Brain Connectivity Toolbox (Rubinov and Sporns, 2010).

Whole-Brain Parcellation—The first step of a topological analysis is to parcellate the brain into functional regions. To accomplish this, we used a previously published atlas of 264 regions classified according to their putative functionality via a meta-analysis of task and resting-state imaging studies (Power et al., 2011). Spherical ROIs (5 mm radius) were centered on coordinates provided by the atlas. ROIs with “unknown” functionality as defined by this analysis were not included, nor those spheres that overlapped with white matter or CSF. We then combined this atlas with the three salience network ROIs (ACC, left and right insula), removing any ROIs from the Power et al. (2011) atlas that overlapped with the ICA-extracted ROIs. Taken together, these ROIs represent “nodes” that constitute a “graph” for which betweenness centrality can be analyzed. It is worthwhile to note that, as previously alluded to in Section 2.5 (“**Functional Connectivity Analysis**”), a limitation of using this type of atlas-based approach is that it requires prespecification of node coordinates. Nonetheless, we considered this method appropriate for the present analysis because we were interested in analyzing topology between salience network nodes and the rest of the brain (or, in the case of local efficiency, topologically adjacent neighbors) as a whole, but not between salience network nodes and specific brain areas.

Time Series Extraction—Functional time series were then extracted by taking the mean signal over time from within each node. Time series were detrended, bandpass filtered, and

white matter/CSF/motion confounders removed as described in ***Functional Connectivity Analysis:*** *Preprocessing*. Analysis was conducted with and without motion censoring as also described in ***Functional Connectivity Analysis:*** *Preprocessing*.

Correlation Matrix Construction—Correlation matrices (i.e., connectivity matrices) for each subject were generated by calculating the absolute value of the Fisher transformation of the correlation in BOLD signal over time (the time series) between each pair of nodes. The diagonal elements of each matrix were set to zero to assure compliance with Brain Connectivity Toolbox functions.

Cost Thresholding and Graph Construction—In a graph theory-based framework, edges between nodes represent "real" connections. Conversely, the absence of an edge between nodes represents the lack of a connection (or "spurious" connection) between them. In order to construct such graphs, cost-based thresholding is performed in which an edge is only placed between nodes with connectivity stronger than the threshold (e.g. the strongest 10% of possible of connections). The procedure is termed "cost" based thresholding because as the connectivity threshold decreases, the number of connections increases, increasing the wiring or topological cost needed in order to construct the graph. As there is no universally accepted threshold that best represents the brain's "true" connections while ignoring "spurious" connections, graph-based metrics were calculated from individual subject graphs across a range of thresholds. Specifically, we calculated betweenness centrality and local efficiency from graphs thresholded from 10% to 50% of possible connections (based on connectivity strength) and ignoring all weaker connections. This range was used because 1) a cost of 10% is typically the lowest cost of a fully connected brain network and 2) connections weaker than the strongest 50% are likely to be non-neuronal and/or strongly influenced by noise (Achard and Bullmore, 2007; Kaiser and Hilgetag, 2006). This cost range is also consistent with previous graph theory-based fMRI studies from our lab and others (Berman et al., 2016; Bullmore and Bassett, 2011; Whitlow et al., 2011). Metrics from each threshold were then integrated over the cost range in order to provide a "cost-integrated" value for each subject to be used for group analyses.

Analyses were performed using both binary and weighted graphs. For binary graphs, all potential connections that met the cost threshold were set to 1 (connection exists) and all other potential connections set to 0 (connection does not exist). For weighted graphs, connectivity strength was preserved for all connections above the cost threshold and all other potential connections set to 0. In graph theory, a "path" is a sequence of edges (i.e. connections) that connect a sequence of nodes (e.g. ROIs). The length of a path between nodes is the topological distance between them. For binary graphs, this is simply the number of nodes along the path between a starting node and the destination node, as the distance between any two adjacently connected nodes is 1. For weighted graphs, the distance between two adjacent nodes is proportional to the connectivity strength between them.

Topological Measures—Betweenness centrality and local efficiency were calculated using functions from the BCT. As suggested by the toolbox, betweenness centrality scores at each cost threshold were normalized such that individual subject values for each salience

network node ranged between 0 and 1. Additional details regarding these measures, including mathematical formalism, can be found in Networks by Newman (2010).

Statistical Analysis—Cost-integrated betweenness centrality and local efficiency scores at the three 5 mm radius salience network nodes (ACC, left and right insula) for each subject and treatment condition were entered into separate mixed model ANOVAs with treatment condition (placebo vs. nicotine) as a within-subjects factor and diagnosis (control vs. patient) as a between-subjects factor. To fully characterize interaction effects, significant interactions were followed up by post-hoc tests of simple main effects. The procedure was conducted for 1) binary graphs without movement censoring, 2) weighted graphs without movement censoring, 3) binary graphs with movement censoring, and 4) weighted graphs with movement censoring.

Correlation Analyses

Connectivity (mean between each seed and significant cluster) and topological metrics for each patient were tested with a Pearson's correlation coefficient for relationships with symptoms (BPRS, SANS, GAF) and global functioning. Correlations with subscales (e.g. SANS Alogia) were only examined if a significant association was observed between the corresponding total score on a scale (e.g. SANS Total) and fMRI-related metrics. Due to the low sample size, we used a liberal significance threshold in which correlations with $p < 0.05$ were considered significant. These analyses should therefore be considered exploratory.

Results

Physiological Effects of Nicotine

Physiological effects of nicotine are presented in Table 2. Physiological data were not available from one control subject due to an equipment malfunction. No significant time X drug X diagnosis interactions were observed for systolic BP ($F(1,33) = 0.55$, $p = 0.47$), diastolic BP ($F(1,33) = 2.01$, $p = 0.17$), or heart rate ($F(1,33) = 0.060$, $p = 0.81$). Across all subjects, no significant time (pretreatment vs. 60 m post-treatment) X drug interactions were observed for systolic BP ($F(1,34) = 2.74$, $p = 0.11$) or diastolic BP ($F(1,34) = 0.22$, $p = 0.64$). A trend-level interaction was observed for heart rate $F(1,34) = 3.92$, $p = 0.056$).

Whole-Brain Seed to Voxel Connectivity Analysis

To understand how nicotine affects connectivity between the salience network and the rest of the brain, 5 mm radius spherical ROIs were centered on salience network peaks extracted by ICA (ACC, left insula, and right insula; see Methods for coordinates) and used for whole brain seed-to-voxel connectivity analysis (see Methods).

Seed-to-Voxel Connectivity Results: ACC Seed—The directional interaction contrast (Patient Nicotine > Patient Placebo) > (Control Nicotine > Control Placebo) yielded significant clusters in the left superior parietal lobule (peak coordinates $\{x, y, z\} = \{-39, -58, 64\}$, $q_{FDR} = 0.004$, cluster size = 209 voxels) and right ventrolateral prefrontal cortex (VLPFC) (peak coordinates $\{x, y, z\} = \{54, 38, 4\}$, $q_{FDR} = 0.004$, cluster size = 194 voxels) (Fig. 3). Post-hoc tests revealed significant interaction effects were driven by decreased

connectivity in patients (vs. controls) under placebo conditions, decreased connectivity in controls under nicotine administration (vs. placebo), and increased connectivity in patients under nicotine administration (vs. placebo) (Fig. 3; Table 3a). Using the opposite directional interaction contrast (Patient Placebo > Patient Nicotine) > (Control Placebo > Control Nicotine) a cluster was observed in the posterior cingulate that approached but did not meet criterion for significance (peak coordinates {*x, y, z*} = {−9, −58, 25}, q_{FDR} = 0.023, cluster size = 159 voxels).

Seed-to-Voxel Connectivity Results: Left Insula Seed—The directional interaction contrast (Patient Placebo > Patient Nicotine) > (Control Placebo > Control Nicotine) yielded a significant cluster in the middle cingulate cortex (MCC) (peak coordinates {*x, y, z*} = {15, −22, 52}, q_{FDR} < 0.001, cluster size = 413 voxels) (Fig. 4). Post-hoc tests revealed the effects were driven by increased connectivity in patients (vs. controls) under placebo conditions, increased connectivity in controls under nicotine administration (vs. placebo), and decreased connectivity in patients under nicotine administration (vs. placebo) (Table 3b). The opposite interaction contrast did not yield any significant effects.

Seed-to-Voxel Connectivity Results: Right Insula Seed—No significant drug X diagnosis interaction effects were observed on connectivity between the right insula seed and remainder of the brain.

Graph Analysis – Binary Graphs

Drug X diagnosis interaction effects on betweenness centrality were analyzed at each salience network node using cost-thresholded binary graphs. Betweenness centrality was cost-integrated over a range of 10% to 50% of possible connections (see Methods). A significant interaction was observed on betweenness centrality in the ACC ($F(1,34) = 10.44$, $p = 0.003$), driven by decreased centrality in patients (vs. controls) under placebo administration ($p = 0.008$), and increased centrality in patients under nicotine administration (vs. placebo ($p = 0.014$) (Fig. 5, top half). No significant interaction effects or main effects of drug were observed on betweenness centrality for either the left or right insula node (Fig. 5, top half). No significant drug X diagnosis interactions were observed for local efficiency of subgraphs centered on any ROI (Table 4a).

Graph Analysis – Weighted Graphs

To determine if graph theory-based results were influenced by connectivity strength and to increase the generalizability of the findings, analyses were repeated using cost-thresholded weighted graphs. Results were similar to the previous analysis using binary graphs. Specifically, a significant drug X diagnosis interaction was observed on betweenness centrality of the ACC ($F(1,34) = 9.95$, $p = 0.003$), driven by decreased centrality in patients (vs. controls) under placebo administration ($p = 0.001$) and increased centrality in patients under nicotine administration (vs. placebo ($p = 0.013$) (Fig. 5, bottom half). No significant interaction effects or main effects of drug were observed on betweenness centrality for either the left or right insula node (Fig. 5, bottom half). No significant drug X diagnosis interactions were observed for local efficiency of subgraphs centered on any ROI (Table 4b).

Clinical Correlates

Connectivity between the left insula and MCC during placebo administration was associated with higher total SANS score (i.e. more severe negative symptoms) in schizophrenia ($r = 0.55$, $p = 0.024$, Fig. 6, top). The effect was primarily driven by an association between connectivity and SANS Anhedonia/Asociality ($r = 0.57$, $p = 0.017$). A positive correlation was observed between connectivity between the ACC and VLPFC during placebo administration in patients and higher GAF score ($r = 0.54$, $p = 0.026$, Fig. 6, bottom). Hypoconnectivity between these areas in patients, therefore, predicted lower global functioning.

Discussion

In agreement with our hypothesis, significant drug X diagnosis interactions were observed between the ACC node of the salience network and brain areas associated with the executive (prefrontal cortex and superior parietal lobule) network. A drug x diagnosis interaction effect between the ACC and PCC approached but not reach significance. A significant drug X diagnosis interaction was also observed between the insula and the MCC. In regards to graph theory-based metrics, a significant interaction effect was observed on betweenness centrality of the ACC node. No significant interactions were observed on betweenness centrality of the insula nodes, however, or for local efficiency of subgraphs centered on any salience network nodes. Significant effects were driven by relative hypoconnectivity (between the ACC and executive regions) and reduced betweenness centrality in patients during placebo administration, and amelioration of these abnormalities after nicotine administration. Hypoconnectivity between the ACC and VLPFC during placebo administration predicted lower global functioning in patients. Furthermore, hyperconnectivity between the insula and MCC predicted severity of negative symptoms including asociality in patients. These results suggest that abnormal connectivity and centrality of the salience network (particularly the ACC component) may be targeted by nicotinic agonists in schizophrenia.

The pattern of connectivity abnormalities observed in the present study suggests that the ACC node of the salience network may be hypoconnected to executive-network areas (e.g. the superior parietal lobule) during the resting state in schizophrenia. This finding is consistent with previous resting state fMRI studies demonstrating hypoconnectivity between the salience network and executive network-associated brain regions in schizophrenia and schizophrenia-associated populations (Chen et al., 2016; Cui et al., 2015; Manoliu et al., 2014; Wang et al., 2015). In contrast to these findings, however, other studies have shown either hyperconnectivity between the salience network and executive regions (Manoliu et al., 2013) or no significant difference in connectivity (Woodward et al., 2011; Wotruba et al., 2014). These discrepancies may be attributed to small sample sizes (Manoliu et al., 2013), the location of seed regions, and different subject populations (e.g. unmedicated at-risk populations (Wotruba et al., 2014)). It should also be noted that the majority of these studies examined connectivity between the insula nodes of the salience network and other networks; this study is one of the first to examine connectivity between a salience network-extracted ACC node and other areas in schizophrenia.

In addition to connectivity, nicotine targeted aberrant centrality of the ACC node of the salience network. In contrast, no interaction effect was observed on local efficiency around any salience network node. This result suggests that nicotinic agonists may affect topological organization of the salience network in schizophrenia on a global, integrative level (as opposed to a local level). Previous work has demonstrated that the salience network has relatively high betweenness centrality, contributing to its ability to act as an indispensable brain "hub" (Cole et al., 2010; Lavin et al., 2013; van den Heuvel and Sporns, 2011). Previous work has also demonstrated that salience network centrality may be disrupted in schizophrenia and in populations at risk for the illness (Crossley et al., 2014; Lord et al., 2012; Lord et al., 2011; van den Heuvel et al., 2010). As a theorized function of the salience network is to integrate information from other major brain networks (Menon, 2015) and betweenness centrality is a surrogate measure of a region's capacity for this process, the results of this study suggest that nicotine may topologically reorganize brain function by restoring salience network integrity. The hypothesized role of the salience network in switching between task-positive and task-negative network-dominant states as a function of cognitive demands (Menon, 2011; Palaniyappan and Liddle, 2012) suggests that nicotine may improve cognition in schizophrenia (Barr et al., 2008; Harris et al., 2004) via its ability to increase the integrative capacity of the network. As cognition was not measured as part of this study, future studies may examine the relationships between salience network connectivity and performance in various cognitive domains.

Notably, nicotine largely had the opposite effect in controls vs. patients; specifically, the drug decreased connectivity between the ACC and executive regions, and decreased ACC betweenness centrality. A possible explanation for the difference in results may be pharmacologic: specifically, controls may have "normal" levels of nicotinic signaling under placebo conditions, and acute nicotine may therefore simply increase receptor desensitization and reduce nicotinic signaling closer to the reduced levels found in patients. Such "inverted U" shaped responses are characteristic of cholinergic as well as other neurotransmitter-based systems (Bentley et al., 2011).

The ability of nicotine to affect betweenness centrality of the ACC may be related to the presence of specialized neurons in the area called *von Economo* or "spindle" neurons. Von Economo neurons are unusually long (160–200 microns or more) neurons that are exclusively present in the ACC and insular cortices of large-brained mammals such as elephants, whales, great apes and humans (Butti et al., 2013). The unique morphology of these cells is thought to enable these brain areas to communicate with distal sites, facilitating their ability to integrate information from many sources to aid in complex computations associated with high-level cognitive functions, e.g. social behavior (Butti et al., 2013). Interestingly, Brune et al. (2010) reported a reduction in density of these neurons in the ACC in schizophrenia patients, as well as inverse associations between von Economo neuron density, illness onset, and length of illness. It is unknown, however, if loss of von Economo neuron signaling is associated with symptomatology or can be pharmacologically targeted by nicotine or other agents to affect network function.

A significant association was noted between left insula – MCC connectivity during placebo administration and negative symptoms in schizophrenia patients, driven primarily by the

Anhedonia/Asociality subscale of the SANS. This subscale measures the degree to which a patient shows relationships with friends and peers (among other factors) (Andreasen, 1983). Related to this finding, social information processing may depend on the MCC. Research in non-human primates has demonstrated that MCC lesions impair social cognition and reduce contact with others (Hadland et al., 2003; Rudebeck et al., 2006). In humans, the MCC is recruited during tasks that involve monitoring the consequences of actions taken by others and may therefore predict outcomes during social interaction (Apps et al., 2013a; Apps et al., 2013b; Behrens et al., 2008). Consequently, it is reasonable to suggest that the MCC is dysfunctional in diseases that feature social cognitive deficits (Apps et al., 2013b). In regards to the present study, the finding that hyperconnectivity between the MCC and insula predicted anhedonia/asociality in patients combined with the result that nicotine targeted this functional abnormality suggests that targeting this circuit via nicotinic agents may have therapeutic benefit. Indeed, one behavioral study observed improved social cognition after acute nicotine administration in nonsmoking schizophrenia patients (Quisenaerts et al., 2013). Another study, however, found no neuronal or behavioral effects of the drug during social cognition in the illness (Drusch et al., 2013). As this area remains understudied, additional research is needed to clarify the role of the MCC in social cognition deficits in schizophrenia as well as to examine the ability of nicotine and other drugs to target the associated circuitry.

A potential limitation of this study is that nicotine can have physiological effects that may reduce the effectiveness of the blind (Benowitz, 1998). It should be noted, however, that 1) nicotine did not have any significant effects on blood pressure or heart rate during scanning in this study, and 2) subjects most likely to have noticeably adverse reactions to nicotine were excluded by prescreening (see Methods). In addition, to help preserve the blind placebo and nicotine patches were covered by clothing, tactilely identical and visually similar, and subjects instructed to refrain from examining the patches. Although it was somewhat surprising to not observe significant physiological effects of the drug, previous work has found only small physiological effects of 7 mg transdermal nicotine (vs. placebo) in nonsmokers up to 120 minutes post-treatment (Wignall and de Wit, 2011). The latent period (resting state scans acquired approximately 120 minutes post-patch application) was chosen as it was expected to capture the peak plasma absorption of nicotine (Dempsey et al., 2013). It remains possible, however, that later time points may show more profound physiological as well as neuronal effects, and it should be acknowledged that lack of a physiological drug effect can be considered a potential limitation of the study. A second limitation is that nicotine levels were not measured as part of this study. Nicotine absorption and metabolism may vary between individuals, potentially making effects more heterogeneous (Ahijevych, 1999; Benowitz et al., 1997). It is also possible that the placebo itself may have had affects on connectivity (relative to a treatment-free state), or that intrinsic connectivity may have affected placebo response (Sikora et al., 2016). Other potential limitations include the relatively small sample size and somewhat arbitrary choice of cost thresholds (from 0.1 to 0.5). It should be noted, however, that the selected cost threshold is well in-line with previous studies (Berman et al., 2016; Bullmore and Bassett, 2011; Whitlow et al., 2011), and is designed to encapsulate fully connected networks that are not unduly influenced by spurious connections (i.e. noise) (see Methods).

Only nonsmoking subjects were examined in this study in order to avoid the potential confounding effects of nicotine withdrawal. It is possible, however, that the effects of nicotine may differ in smoking patients. Indeed, chronic smoking is associated with increased expression of nicotinic receptors in both schizophrenia patients and healthy subjects (Esterlis et al., 2014; Mexal et al., 2010; Mukhin et al., 2008), suggesting that responsiveness to nicotine may differ between smokers and nonsmokers. Related to this point, as is typical of studies that examine schizophrenia patients the observed effects may have been confounded by use of antipsychotics. Reduced connectivity between the ACC and insula, for example, has been previously observed during a salience attribution task in untreated (first-episode) patients relative to (atypical antipsychotic) medicated patients (Schmidt et al., 2016). A number of patients who participated in this study were taking clozapine, which has been shown to reduce smoking in schizophrenia (McEvoy et al., 1995) possibly by interfering with cholinergic transmission (Singhal et al., 2007). The effect of nicotine on the connectivity measures in this study in smoking and antipsychotic-naive populations are important areas for future study.

The ability of nicotinic agents to pharmacologically target intrinsic network dysfunction in schizophrenia remains a priority for psychiatry research. This study identifies functional salience network abnormalities as potential nicotinic targets in schizophrenia. Future imaging studies may investigate the ability of nicotine and nicotinic agonists to target this network as well as other areas that highly express nicotinic receptors (such as the striatum and hippocampus) in additional schizophrenia and schizophrenia-related populations.

Supplementary Material

Refer to Web version on PubMed Central for supplementary material.

Acknowledgments

The authors thank Debra Singel for help with data acquisition. This work was supported by the VA Biomedical Laboratory and Clinical Science Research and Development Service grant CX000459 (grant to Dr. Tregellas), the Brain and Behavior Research Foundation (grant to Dr. Tregellas), NIH grants MH-089095, DK-103691, MH-102224 (grants to Dr. Tregellas), and NIH fellowship MH-102879 (grant to Mr. Smucny).

References

Achard S, Bullmore E. Efficiency and cost of economical brain functional networks. PLoS Comp Biol. 2007; 3:174–83.

Ahijevych K. Nicotine metabolism variability and nicotine addiction. Nicotine Tob Res. 1999; 1(Suppl 2):S59–62. discussion S9–70.

Andreasen, N. The scale for the assessment of negative symptoms (SANS). Iowa City: University of Iowa; 1983.

Apps MA, Green R, Ramnani N. Reinforcement learning signals in the anterior cingulate cortex code for others' false beliefs. Neuroimage. 2013a; 64:1–9. [PubMed: 22982355]

Apps MA, Lockwood PL, Balsters JH. The role of the midcingulate cortex in monitoring others' decisions. Front Neurosci. 2013b; 7:251. [PubMed: 24391534]

Barr RS, Culhane MA, Jubelt LE, Mufti RS, Dyer MA, Weiss AP, et al. The effects of transdermal nicotine on cognition in nonsmokers with schizophrenia and nonpsychiatric controls. Neuropsychopharmacology. 2008; 33:480–90. [PubMed: 17443126]

Behrens TE, Hunt LT, Woolrich MW, Rushworth MF. Associative learning of social value. Nature. 2008; 456:245–9. [PubMed: 19005555]

Bell AJ, Sejnowski TJ. An information-maximization approach to blind separation and blind deconvolution. Neural Comput. 1995; 7:1129–59. [PubMed: 7584893]

Benowitz, NL. Nicotine Safety and Toxicity. New York, NY: Oxford University Press; 1998.

Benowitz NL, Zevin S, Jacob P 3rd. Sources of variability in nicotine and cotinine levels with use of nicotine nasal spray, transdermal nicotine, and cigarette smoking. Br J Clin Pharmacol. 1997; 43:259–67. [PubMed: 9088580]

Bentley P, Driver J, Dolan RJ. Cholinergic modulation of cognition: insights from human pharmacological functional neuroimaging. Prog Neurobiol. 2011; 94:360–88. [PubMed: 21708219]

Berman BD, Smucny J, Wylie KP, Shelton E, Kronberg E, Leehey M, et al. Levodopa modulates small-world architecture of functional brain networks in Parkinson's disease. Mov Disord. 2016; 31:1676–84. [PubMed: 27461405]

Breese CR, Adams C, Logel J, Drebing C, Rollins Y, Barnhart M, et al. Comparison of the regional expression of nicotinic acetylcholine receptor alpha7 mRNA and [125I]-alpha-bungarotoxin binding in human postmortem brain. J Comp Neurol. 1997; 387:385–98. [PubMed: 9335422]

Brune M, Schobel A, Karau R, Benali A, Faustmann PM, Juckel G, et al. Von Economo neuron density in the anterior cingulate cortex is reduced in early onset schizophrenia. Acta Neuropathol. 2010; 119:771–8. [PubMed: 20309567]

Bullmore ET, Bassett DS. Brain graphs: graphical models of the human brain connectome. Annu Rev Clin Psychol. 2011; 7:113–40. [PubMed: 21128784]

Butti C, Santos M, Uppal N, Hof PR. Von Economo neurons: clinical and evolutionary perspectives. Cortex. 2013; 49:312–26. [PubMed: 22130090]

Chen Q, Chen X, He X, Wang L, Wang K, Qiu B. Aberrant structural and functional connectivity in the salience network and central executive network circuit in schizophrenia. Neurosci Lett. 2016; 627:178–84. [PubMed: 27233217]

Cole MW, Pathak S, Schneider W. Identifying the brain's most globally connected regions. Neuroimage. 2010; 49:3132–48. [PubMed: 19909818]

Cosgrove KP, Batis J, Bois F, Maciejewski PK, Esterlis I, Kloczynski T, et al. beta2-Nicotinic acetylcholine receptor availability during acute and prolonged abstinence from tobacco smoking. Arch Gen Psychiatry. 2009; 66:666–76. [PubMed: 19487632]

Crossley NA, Mechelli A, Scott J, Carletti F, Fox PT, McGuire P, et al. The hubs of the human connectome are generally implicated in the anatomy of brain disorders. Brain. 2014; 137:2382–95. [PubMed: 25057133]

Cui LB, Liu J, Wang LX, Li C, Xi YB, Guo F, et al. Anterior cingulate cortex-related connectivity in first-episode schizophrenia: a spectral dynamic causal modeling study with functional magnetic resonance imaging. Front Hum Neurosci. 2015; 9:589. [PubMed: 26578933]

Dempsey DA, St Helen G, Jacob P 3rd, Tyndale RF, Benowitz NL. Genetic and pharmacokinetic determinants of response to transdermal nicotine in white, black, and Asian nonsmokers. Clin Pharmacol Ther. 2013; 94:687–94. [PubMed: 23933970]

Dodhia S, Hosanagar A, Fitzgerald DA, Labuschagne I, Wood AG, Nathan PJ, et al. Modulation of resting-state amygdala-frontal functional connectivity by oxytocin in generalized social anxiety disorder. Neuropsychopharmacology. 2014; 39:2061–9. [PubMed: 24594871]

Drusch K, Lowe A, Fisahn K, Brinkmeyer J, Musso F, Mobascher A, et al. Effects of nicotine on social cognition, social competence and self-reported stress in schizophrenia patients and healthy controls. Eur Arch Psychiatry Clin Neurosci. 2013; 263:519–27. [PubMed: 23081705]

Esterlis I, Ranganathan M, Bois F, Pittman B, Picciotto MR, Shearer L, et al. In vivo evidence for beta2 nicotinic acetylcholine receptor subunit upregulation in smokers as compared with nonsmokers with schizophrenia. Biol Psychiatry. 2014; 76:495–502. [PubMed: 24360979]

Genovese CR, Lazar NA, Nichols T. Thresholding of statistical maps in functional neuroimaging using the false discovery rate. Neuroimage. 2002; 15:870–8. [PubMed: 11906227]

Hadland KA, Rushworth MF, Gaffan D, Passingham RE. The effect of cingulate lesions on social behaviour and emotion. Neuropsychologia. 2003; 41:919–31. [PubMed: 12667528]

Harris JG, Kongs S, Allensworth D, Martin L, Tregellas J, Sullivan B, et al. Effects of nicotine on cognitive deficits in schizophrenia. Neuropsychopharmacology. 2004; 29:1378–85. [PubMed: 15138435]

Hong LE, Gu H, Yang Y, Ross TJ, Salmeron BJ, Buchholz B, et al. Association of nicotine addiction and nicotine's actions with separate cingulate cortex functional circuits. Arch Gen Psychiatry. 2009; 66:431–41. [PubMed: 19349313]

Jones SH, Thornicroft G, Coffey M, Dunn G. A brief mental health outcome scale-reliability and validity of the Global Assessment of Functioning (GAF). Br J Psychiatry. 1995; 166:654–9. [PubMed: 7620753]

Kaiser M, Hilgetag CC. Nonoptimal component placement, but short processing paths, due to long-distance projections in neural systems. PLoS Comput Biol. 2006; 2:e95. [PubMed: 16848638]

Kelly RE, Wang Z, Alexopoulos GS, Gunning FM, Murphy CF, Morimoto SS, et al. Hybrid ICA-Seed-Based Methods for fMRI Functional Connectivity Assessment: A Feasibility Study. Int J Biomed Imaging. 2010

Kraguljac NV, White DM, Hadley JA, Visscher K, Knight D, ver Hoef L, et al. Abnormalities in large scale functional networks in unmedicated patients with schizophrenia and effects of risperidone. Neuroimage Clin. 2016; 10:146–58. [PubMed: 26793436]

Kriegeskorte N, Simmons WK, Bellgowan PS, Baker CI. Circular analysis in systems neuroscience: the dangers of double dipping. Nat Neurosci. 2009; 12:535–40. [PubMed: 19396166]

Kuhn S, Gallinat J. Quantitative meta-analysis on state and trait aspects of auditory verbal hallucinations in schizophrenia. Schizophr Bull. 2012; 38:779–86. [PubMed: 21177743]

Lahti AC, Weiler MA, Holcomb HH, Tamminga CA, Carpenter WT, McMahon R. Correlations between rCBF and symptoms in two independent cohorts of drug-free patients with schizophrenia. Neuropsychopharmacology. 2006; 31:221–30. [PubMed: 16123774]

Lavin C, Melis C, Mikulan E, Gelormini C, Huepe D, Ibanez A. The anterior cingulate cortex: an integrative hub for human socially-driven interactions. Front Neurosci. 2013; 7:64. [PubMed: 23658536]

Lord LD, Allen P, Expert P, Howes O, Broome M, Lambiotte R, et al. Functional brain networks before the onset of psychosis: A prospective fMRI study with graph theoretical analysis. Neuroimage Clin. 2012; 1:91–8. [PubMed: 24179741]

Lord LD, Allen P, Expert P, Howes O, Lambiotte R, McGuire P, et al. Characterization of the anterior cingulate's role in the at-risk mental state using graph theory. Neuroimage. 2011; 56:1531–9. [PubMed: 21316462]

Manoliu A, Riedl V, Doll A, Bauml JG, Muhlau M, Schwerthoffer D, et al. Insular Dysfunction Reflects Altered Between-Network Connectivity and Severity of Negative Symptoms in Schizophrenia during Psychotic Remission. Front Hum Neurosci. 2013; 7:216. [PubMed: 23730284]

Manoliu A, Riedl V, Zherdin A, Muhlau M, Schwerthoffer D, Scherr M, et al. Aberrant dependence of default mode/central executive network interactions on anterior insular salience network activity in schizophrenia. Schizophr Bull. 2014; 40:428–37. [PubMed: 23519021]

McEvoy J, Freudenreich O, McGee M, VanderZwaag C, Levin E, Rose J. Clozapine decreases smoking in patients with chronic schizophrenia. Biol Psychiatry. 1995; 37:550–2. [PubMed: 7619979]

Menon V. Large-scale brain networks and psychopathology: a unifying triple network model. Trends Cogn Sci. 2011; 15:483–506. [PubMed: 21908230]

Menon, V. Salience Network. In: Toga, AW., editor. Brain Mapping: An Encyclopedic Reference. Academic Press: Elsevier; 2015. p. 597-611.

Menon V, Uddin LQ. Saliency, switching, attention and control: a network model of insula function. Brain Struct Funct. 2010; 214:655–67. [PubMed: 20512370]

Mexal S, Berger R, Logel J, Ross RG, Freedman R, Leonard S. Differential regulation of alpha7 nicotinic receptor gene (CHRNA7) expression in schizophrenic smokers. J Mol Neurosci. 2010; 40:185–95. [PubMed: 19680823]

Moran LV, Sampath H, Kochunov P, Hong LE. Brain circuits that link schizophrenia to high risk of cigarette smoking. Schizophr Bull. 2013a; 39:1373–81. [PubMed: 23236076]

Moran LV, Tagamets MA, Sampath H, O'Donnell A, Stein EA, Kochunov P, et al. Disruption of anterior insula modulation of large-scale brain networks in schizophrenia. Biol Psychiatry. 2013b; 74:467–74. [PubMed: 23623456]

Mukhin AG, Kimes AS, Chefer SI, Matochik JA, Contoreggi CS, Horti AG, et al. Greater nicotinic acetylcholine receptor density in smokers than in nonsmokers: a PET study with 2–18F-FA-85380. J Nucl Med. 2008; 49:1628–35. [PubMed: 18794265]

Murphy K, Birn RM, Bandettini PA. Resting-state fMRI confounds and cleanup. Neuroimage. 2013; 80:349–59. [PubMed: 23571418]

Newman, MEJ. Networks. Oxford, U.K: Oxford University Press; 2010.

Palaniyappan L, Liddle PF. Does the salience network play a cardinal role in psychosis? An emerging hypothesis of insular dysfunction. J Psychiatry Neurosci. 2012; 37:17–27. [PubMed: 21693094]

Palaniyappan L, Simmonite M, White TP, Liddle EB, Liddle PF. Neural primacy of the salience processing system in schizophrenia. Neuron. 2013; 79:814–28. [PubMed: 23972602]

Palaniyappan L, White TP, Liddle PF. The concept of salience network dysfunction in schizophrenia: from neuroimaging observations to therapeutic opportunities. Curr Top Med Chem. 2012; 12:2324–38. [PubMed: 23279173]

Paterson D, Nordberg A. Neuronal nicotinic receptors in the human brain. Prog Neurobiol. 2000; 61:75–111. [PubMed: 10759066]

Patriat R, Molloy EK, Meier TB, Kirk GR, Nair VA, Meyerand ME, et al. The effect of resting condition on resting-state fMRI reliability and consistency: a comparison between resting with eyes open, closed, and fixated. Neuroimage. 2013; 78:463–73. [PubMed: 23597935]

Pelletier-Baldelli A, Bernard JA, Mittal VA. Intrinsic Functional Connectivity in Salience and Default Mode Networks and Aberrant Social Processes in Youth at Ultra-High Risk for Psychosis. PLoS One. 2015; 10:e0134936. [PubMed: 26252525]

Picard F, Sadaghiani S, Leroy C, Courvoisier DS, Maroy R, Bottlaender M. High density of nicotinic receptors in the cingulo-insular network. Neuroimage. 2013; 79:42–51. [PubMed: 23631995]

Power JD, Barnes KA, Snyder AZ, Schlaggar BL, Petersen SE. Spurious but systematic correlations in functional connectivity MRI networks arise from subject motion. Neuroimage. 2012; 59:2142–54. [PubMed: 22019881]

Power JD, Cohen AL, Nelson SM, Wig GS, Barnes KA, Church JA, et al. Functional network organization of the human brain. Neuron. 2011; 72:665–78. [PubMed: 22099467]

Pu W, Li L, Zhang H, Ouyang X, Liu H, Zhao J, et al. Morphological and functional abnormalities of salience network in the early-stage of paranoid schizophrenia. Schizophr Res. 2012; 141:15–21. [PubMed: 22910405]

Quisenaerts C, Morrens M, Hulstijn W, de Boer P, Timmers M, Sabbe B, et al. Acute nicotine improves social decision-making in non-smoking but not in smoking schizophrenia patients. Front Neurosci. 2013; 7:197. [PubMed: 24198754]

Roh S, Hoeppner SS, Schoenfeld D, Fullerton CA, Stoeckel LE, Evins AE. Acute effects of mecamylamine and varenicline on cognitive performance in non-smokers with and without schizophrenia. Psychopharmacology (Berl). 2014; 231:765–75. [PubMed: 24114425]

Rubinov M, Sporns O. Complex network measures of brain connectivity: uses and interpretations. Neuroimage. 2010; 52:1059–69. [PubMed: 19819337]

Rudebeck PH, Buckley MJ, Walton ME, Rushworth MF. A role for the macaque anterior cingulate gyrus in social valuation. Science. 2006; 313:1310–2. [PubMed: 16946075]

Schmidt A, Palaniyappan L, Smieskova R, Simon A, Riecher-Rossler A, Lang UE, et al. Dysfunctional insular connectivity during reward prediction in patients with first-episode psychosis. J Psychiatry Neurosci. 2016; 41:367–76. [PubMed: 26854756]

Seeley WW, Menon V, Schatzberg AF, Keller J, Glover GH, Kenna H, et al. Dissociable intrinsic connectivity networks for salience processing and executive control. J Neurosci. 2007; 27:2349–56. [PubMed: 17329432]

Shirer WR, Ryali S, Rykhlevskaia E, Menon V, Greicius MD. Decoding subject-driven cognitive states with whole-brain connectivity patterns. Cereb Cortex. 2012; 22:158–65. [PubMed: 21616982]

Sikora M, Heffernan J, Avery ET, Mickey BJ, Zubieta JK, Pecina M. Salience Network Functional Connectivity Predicts Placebo Effects in Major Depression. Biol Psychiatry Cogn Neurosci Neuroimaging. 2016; 1:68–76. [PubMed: 26709390]

Singhal SK, Zhang L, Morales M, Oz M. Antipsychotic clozapine inhibits the function of alpha7-nicotinic acetylcholine receptors. Neuropharmacology. 2007; 52:387–94. [PubMed: 17161853]

Smucny J, Olincy A, Rojas DC, Tregellas JR. Neuronal effects of nicotine during auditory selective attention in schizophrenia. Hum Brain Mapp. 2016a; 37:410–21. [PubMed: 26518728]

Smucny J, Olincy A, Tregellas JR. Nicotine restores functional connectivity of the ventral attention network in schizophrenia. Neuropharmacology. 2016b; 108:144–51. [PubMed: 27085606]

Smucny J, Stevens KE, Olincy A, Tregellas JR. Translational utility of rodent hippocampal auditory gating in schizophrenia research: a review and evaluation. Transl Psychiatry. 2015; 5:e587. [PubMed: 26101850]

Smucny J, Tregellas J. Nicotinic modulation of intrinsic brain networks in schizophrenia. Biochem Pharmacol. 2013; 86:1163–72. [PubMed: 23796751]

Sridharan D, Levitin DJ, Menon V. A critical role for the right fronto-insular cortex in switching between central-executive and default-mode networks. Proc Natl Acad Sci U S A. 2008; 105:12569–74. [PubMed: 18723676]

Sutherland MT, Carroll AJ, Salmeron BJ, Ross TJ, Hong LE, Stein EA. Down-regulation of amygdala and insula functional circuits by varenicline and nicotine in abstinent cigarette smokers. Biol Psychiatry. 2013; 74:538–46. [PubMed: 23506999]

Sutherland MT, McHugh MJ, Pariyadath V, Stein EA. Resting state functional connectivity in addiction: Lessons learned and a road ahead. Neuroimage. 2012; 62:2281–95. [PubMed: 22326834]

Tregellas JR, Smucny J, Harris JG, Olincy A, Maharajh K, Kronberg E, et al. Intrinsic hippocampal activity as a biomarker for cognition and symptoms in schizophrenia. Am J Psychiatry. 2014; 171:549–56. [PubMed: 24435071]

Tregellas JR, Tanabe J, Rojas DC, Shatti S, Olincy A, Johnson L, et al. Effects of an alpha 7-nicotinic agonist on default network activity in schizophrenia. Biol Psychiatry. 2011; 69:7–11. [PubMed: 20728875]

Uddin LQ, Supekar KS, Ryali S, Menon V. Dynamic reconfiguration of structural and functional connectivity across core neurocognitive brain networks with development. J Neurosci. 2011; 31:18578–89. [PubMed: 22171056]

van den Heuvel MP, Mandl RC, Kahn RS, Hulshoff Pol HE. Functionally linked resting-state networks reflect the underlying structural connectivity architecture of the human brain. Hum Brain Mapp. 2009; 30:3127–41. [PubMed: 19235882]

van den Heuvel MP, Mandl RC, Stam CJ, Kahn RS, Hulshoff Pol HE. Aberrant frontal and temporal complex network structure in schizophrenia: a graph theoretical analysis. J Neurosci. 2010; 30:15915–26. [PubMed: 21106830]

van den Heuvel MP, Sporns O. Rich-club organization of the human connectome. J Neurosci. 2011; 31:15775–86. [PubMed: 22049421]

van den Heuvel MP, Sporns O. Network hubs in the human brain. Trends Cogn Sci. 2013; 17:683–96. [PubMed: 24231140]

Ventura J, Lukoff D, Nuechterlein KH, Liberman RP, Green MF, Shaner A. Appendix 1: Brief Psychiatric Rating Scale (BPRS) Expanded version (4.0) scales, anchor points and administration manual. Int J Methods Psychiatr Res. 1993; 3:227–44.

Wang D, Zhou Y, Zhuo C, Qin W, Zhu J, Liu H, et al. Altered functional connectivity of the cingulate subregions in schizophrenia. Transl Psychiatry. 2015; 5:e575. [PubMed: 26035059]

Wei Z, Yang N, Liu Y, Yang L, Wang Y, Han L, et al. Resting-state functional connectivity between the dorsal anterior cingulate cortex and thalamus is associated with risky decision-making in nicotine addicts. Sci Rep. 2016; 6:21778. [PubMed: 26879047]

Whitlow CT, Casanova R, Maldjian JA. Effect of resting-state functional MR imaging duration on stability of graph theory metrics of brain network connectivity. Radiology. 2011; 259:516–24. [PubMed: 21406628]

Wignall ND, de Wit H. Effects of nicotine on attention and inhibitory control in healthy nonsmokers. Exp Clin Psychopharmacol. 2011; 19:183–91. [PubMed: 21480731]

Winterer G. Why do patients with schizophrenia smoke? Curr Opin Psychiatry. 2010; 23:112–9. [PubMed: 20051860]

Woodward ND, Rogers B, Heckers S. Functional resting-state networks are differentially affected in schizophrenia. Schizophr Res. 2011; 130:86–93. [PubMed: 21458238]

Wotruba D, Michels L, Buechler R, Metzler S, Theodoridou A, Gerstenberg M, et al. Aberrant coupling within and across the default mode, task-positive, and salience network in subjects at risk for psychosis. Schizophr Bull. 2014; 40:1095–104. [PubMed: 24243441]

Wylie KP, Smucny J, Legget KT, Tregellas JR. Targeting Functional Biomarkers in Schizophrenia with Neuroimaging. Curr Pharm Des. 2016; 22:2117–23. [PubMed: 26818860]

Wylie KP, Tregellas JR. The role of the insula in schizophrenia. Schizophr Res. 2010; 123:93–104. [PubMed: 20832997]

Yan H, Tian L, Wang Q, Zhao Q, Yue W, Yan J, et al. Compromised small-world efficiency of structural brain networks in schizophrenic patients and their unaffected parents. Neurosci Bull. 2015; 31:275–87. [PubMed: 25813916]

Zilles K, Amunts K. Centenary of Brodmann's map--conception and fate. Nat Rev Neurosci. 2010; 11:139–45. [PubMed: 20046193]

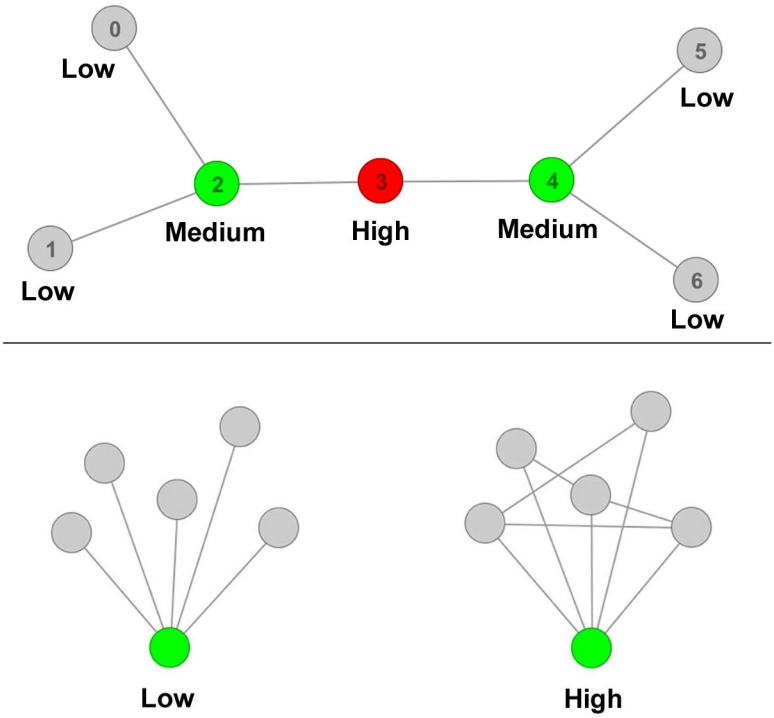

Fig. 1.

Top: Graphical illustration of betweenness centrality. Betweenness centrality is defined as the proportion of shortest paths of a network that contain a given node. Nodes with low betweenness centrality are colored in gray, nodes with medium betweenness centrality colored in green, and the node with the highest betweenness centrality colored in red. Node 3 (the red node) participates in the highest number of shortest paths between each pair of all other nodes in the network and therefore has the highest betweenness centrality. In the present framework, nodes represent brain regions and edges represent connections between regions. *Bottom:* Graphical illustration of local efficiency. Local efficiency is a measure of ability of a node and its neighbors to transfer information between themselves. The graph on the left has low local efficiency of the green node and its neighbors. The graph on the right has high local efficiency of the green node and its neighbors due to increased connections between the neighbors.

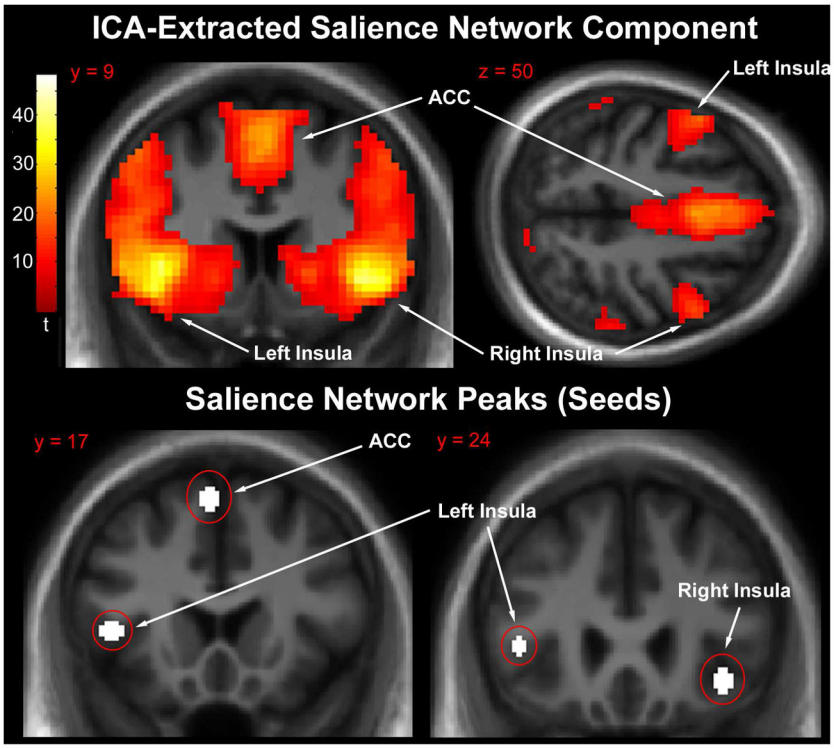

Fig. 2.

Top: Mean salience network component extracted by independent components analysis. Significant clusters were centered on the anterior cingulate and bilateral insula. Statistical parametric map thresholded at whole-brain voxelwise cluster family-wise error rate corrected $p < 0.05$ purely for visualization purposes. Images are presented in the neurologic convention (R on R). *Bottom:* Location of salience network peaks (5 mm spheres) used as seeds for connectivity analysis.

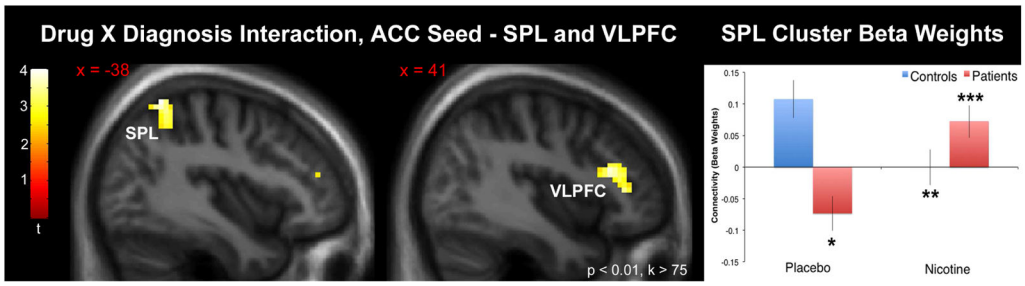

Fig. 3.

Left: Anterior cingulate seed to voxelwise whole-brain connectivity result using the directional drug X diagnosis interaction contrast (Patient Nicotine > Patient Placebo) > (Control Nicotine > Control Placebo). Significant clusters were observed in the superior parietal lobule and ventrolateral prefrontal cortex. Statistical parametric map thresholded at $p < 0.01$, $k > 75$ voxels purely for visualization purposes (significance threshold specified in methods). Images are presented in the neurologic convention (R on R). Abbreviations: ACC – anterior cingulate cortex; SPL – superior parietal lobule; VLPFC – ventrolateral prefrontal cortex.

Right: Chart displaying the nature of the drug X diagnosis interaction. Cluster beta weight values represent the mean taken from the superior parietal lobule cluster. *$p < 0.05$ vs. control placebo (post-hoc test). **$p < 0.05$ vs. control nicotine. ***$p < 0.05$ vs. patient placebo.

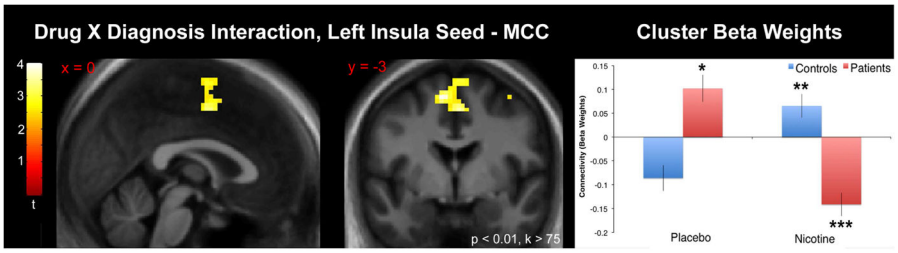

Fig. 4.

Left: Left insula seed to voxelwise whole-brain connectivity result using the directional drug X diagnosis interaction contrast (Patient Placebo > Patient Nicotine) > (Control Placebo > Control Nicotine). A significant cluster was observed in the middle cingulate cortex. Statistical parametric map thresholded at $p < 0.01$, cluster size > 75 voxels purely for visualization purposes (significance threshold specified in methods). Images are presented in the neurologic convention (R on R). Abbreviations: MCC – middle cingulate cortex. *Right:* Chart displaying the nature of the drug X diagnosis interaction. Cluster beta weight values represent the mean taken from the cluster. *$p < 0.05$ vs. control placebo (post-hoc test). **$p < 0.05$ vs. control nicotine. ***$p < 0.05$ vs. patient placebo.

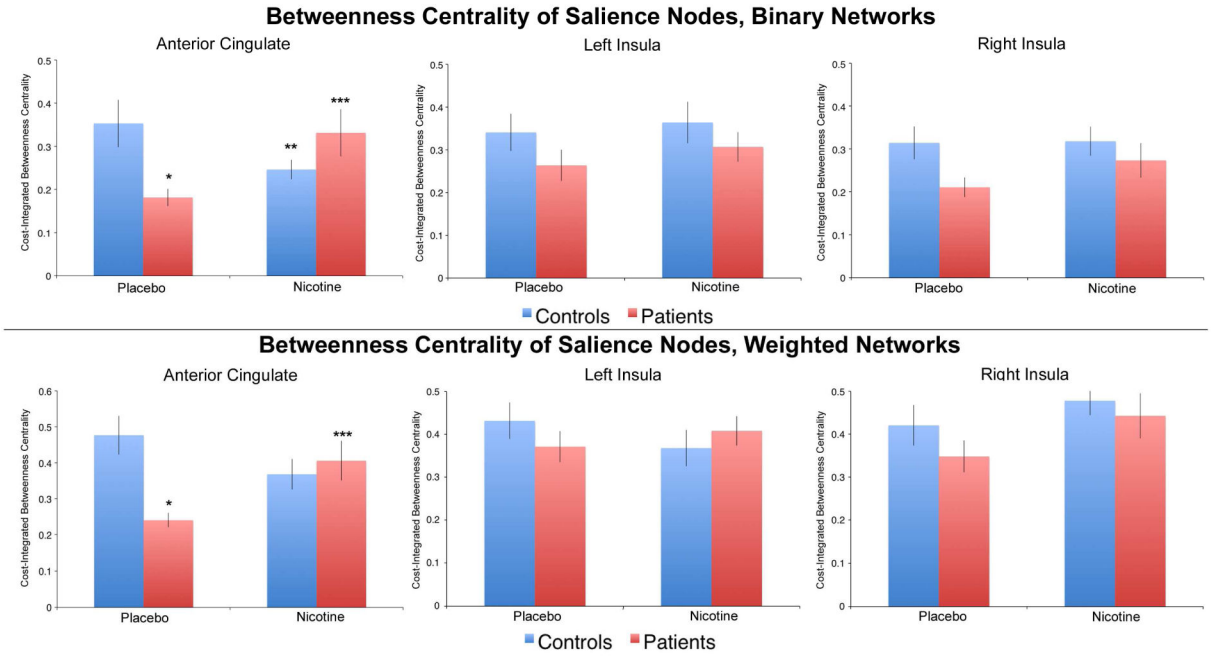

Fig. 5.

Top: Drug x diagnosis interaction effects on betweenness centrality for the anterior cingulate cortex (ACC), left insula, and right insula nodes using binary network analysis. A significant interaction effect was observed for the ACC but not the insula nodes. *$p < 0.05$ vs. control placebo. ** $p < 0.05$ vs. control placebo. ***$p < 0.05$ vs. patient placebo.

Bottom: Drug x diagnosis interaction effects on betweenness centrality for the ACC, left insula, and right insula nodes using weighted network analysis. A significant interaction effect was observed for the ACC but not the insula nodes. . *$p < 0.05$ vs. control placebo. ***$p < 0.05$ vs. patient placebo.

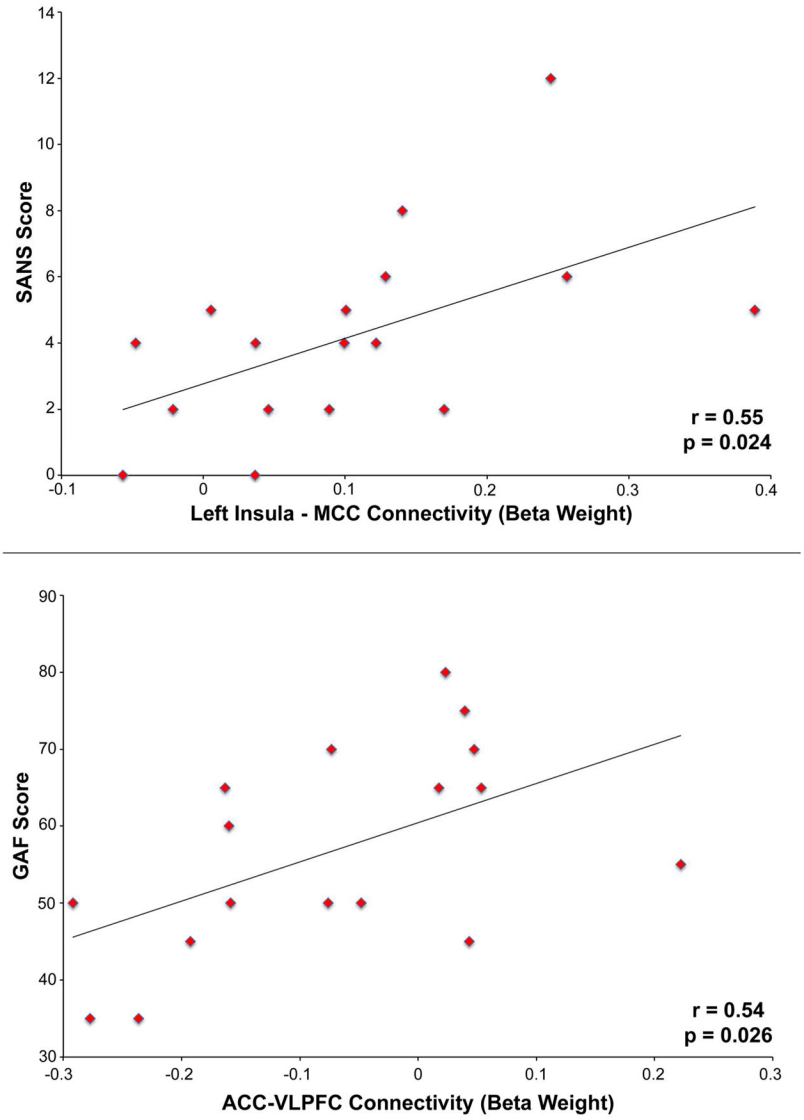

Fig. 6.

Top: Positive correlation between connectivity between the left insula and middle cingulate cortex (MCC) during placebo administration in schizophrenia patients and SANS score. *Bottom:* Positive correlation between connectivity between the anterior cingulate cortex (ACC) and ventrolateral prefrontal cortex (VLPFC) during placebo administration in schizophrenia patients and GAF score.

Table 1

Demographic and Clinical Data of Participants.

	Controls	Schizophrenia	Test Statistic (p)
Age	37.4 (12)	44 (12)	t = 1.61 (0.12)
Gender (M/F)	10/9	12/5	X^2 = 1.22 (0.32)
Average Total BPRS		36.6 (7.7)	n/a
Average Total SANS		4.59 (3.4)	n/a
Meds: Typ/ATyp		1/16	n/a

Parentheses contain the standard deviation. Abbreviations: BPRS = Brief Psychiatric Rating Scale, SANS = Scale for the Assessment of Negative Symptoms, Typ = # Treated with Typical Antipsychotic Medications, ATyp = # Treated with Atypical Antipsychotic Medications.

Table 2

Physiological effects of nicotine and placebo patch.

	Tx	Placebo			Nicotine		
Group	**Measure**	**Pretreatment**	**60m Posttreatment**	**Δ**	**Pretreatment**	**60m Posttreatment**	**Δ**
Controls	**Systolic BP (mmHg)**	129 (4)	121 (4)	−8 (2)	128 (3)	125 (2)	−2 (2)
	Diastolic BP (mmHg)	79 (2)	76 (2)	−3 (2)	79 (2)	80 (2)	1 (2)
	Heart Rate (bpm)	73 (2)	70 (2)	−3 (2)	76 (3)	76 (3)	0 (1)
Schizophrenia Patients	**Systolic BP (mmHg)**	135 (4)	130 (4)	−5 (5)	128 (4)	125 (3)	−3 (2)
	Diastolic BP (mmHg)	79 (2)	79 (3)	0 (2)	80 (2)	78 (2)	−2 (2)
	Heart Rate (bpm)	81 (4)	81 (4)	0 (2)	84 (4)	87 (4)	3 (2)

Parentheses contain the standard error. Abbreviations: BP = blood pressure, mmHg = mm of mercury, bpm = beats per minute.

Table 3a

Connectivity (beta weights) between the ACC seed and significant clusters drawn from whole-brain drug X diagnosis interaction contrasts. *P* values are drawn from post-hoc tests of simple main effects (see Methods) and are displayed to describe the nature of the interactions.

Brain Region	**Controls**			**Patients**			
	Placebo	**Nicotine**	***p* (nicotine vs. placebo)**	**Placebo**	**Nicotine**	***p* (patient vs. control placebo)**	***p* (nicotine vs. placebo)**
SPL	0.11 (0.03)	−0.0020 (0.03)	0.001	−0.07 (0.03)	0.07 (0.03)	< 0.001	< 0.001
VLPFC	0.06 (0.03)	−0.08 (0.03)	0.001	−0.07 (0.03)	0.08 (0.04)	0.004	< 0.001

Values in parentheses represent the standard error. Abbreviations: SPL – superior parietal lobule, VLPFC – ventrolateral prefrontal cortex.

Table 3b

Connectivity (beta weights) between the left insula seed and the significant cluster drawn from whole-brain drug X diagnosis interaction contrasts. *P* values are drawn from post-hoc tests of simple main effects (see Methods) and are displayed to describe the nature of the interaction.

Brain Region	Controls			Patients			
	Placebo	Nicotine	*p* (nicotine vs. placebo)	Placebo	Nicotine	*p* (patient vs. control placebo)	*p* (nicotine vs. placebo)
MCC	−0.09 (0.03)	0.07 (0.02)	< 0.001	0.10 (0.03)	−0.14 (0.02)	< 0.001	< 0.001

Values in parentheses represent the standard error. Abbreviations: MCC – middle cingulate cortex.

Table 4a

Local efficiency of binary subgraphs centered on each salience network node.

Brain Region	Controls		Patients	
	Placebo	Nicotine	Placebo	Nicotine
ACC	0.30 (0.01)	0.31 (0.01)	0.30 (0.02)	0.32 (0.008)
Left Insula	0.31 (0.01)	0.31 (0.01)	0.32 (0.007)	0.29 (0.01)
Right Insula	0.31 (0.01)	0.32 (0.005)	0.31 (0.02)	0.32 (0.008)

Abbreviations: ACC – anterior cingulate cortex. Values in parentheses represent the standard error.

Table 4b

Local efficiency of weighted subgraphs centered on each salience network node.

Brain Region	Controls		Patients	
	Placebo	Nicotine	Placebo	Nicotine
ACC	0.33 (0.03)	0.37 (0.04)	0.38 (0.04)	0.39 (0.03)
Left Insula	0.35 (0.03)	0.36 (0.02)	0.41 (0.03)	0.34 (0.03)
Right Insula	0.36 (0.03)	0.39 (0.03)	0.39 (0.04)	0.37 (0.02)

Abbreviations: ACC – anterior cingulate cortex. Values in parentheses represent the standard error.